Supporting Information

Hayashi-Takagi et al. 10.1073/pnas.1321109111

SI Materials and Methods

Whole-cell recordings were made from cortical cultures. Small fire-polished patch electrodes (7–9 MΩ) were used to prevent washing out cellular components required for long-term potentiation (LTP) induction. The series resistance in these recordings varied between 30 and 35 MΩ, and datasets where series resistance varied more than 10% during the recording were rejected for further analysis. No electronic compensations for series resistance were used. The patch electrode solution contained the following (mM): $CsMeSO_4$, 115; EGTA, 0.4; TEA-Cl, 5; NaCl, 2.8; Hepes, 20; Mg-ATP, 3: Na-GTP, 0.5; Na-Phosphocreatine, 10 (pH 7.2); and osmolarity between 290 and 292 $mosmol^{-1}$. The extracellular solution (ECS) composition contained the following (mM): NaCl, 143; KCl, 5; Hepes, 10; Glucose, 10; $CaCl_2$ 2; tetrodotoxin, 0.0005; strychnine, 0.001; picrotoxin, 0.1 (pH 7.4); and osmolarity between 302 and 305 $mosmol^{-1}$. During the basal recording of miniature excitatory postsynaptic currents and uncaging-evoked excitatory postsynaptic currents (uEPSC), cells were voltage-clumped at −65 mV and perfused with ECS containing 200 mM amino-5-phosphonovaleric acid (APV) (APV-ECS). For chemical LTP induction, cells were maintained at 0 mV and perfused with ECS containing 30 μM *D*-Serine for 10 min. For measuring uEPSC, cells were perfused with APV-ECS supplemented with 5 mM MNI-glutamate (Tocris Bioscience). Two-photon uncaging laser (720 nm: mode-locked Ti-Sapphire laser) was delivered to the spine head to photolyse the caged-glutamate for 2 ms. Intensity of uncaging laser was 20 mW at the back aperture of the objective lens. Duration and intensity of uncaging laser were controlled by electro-optic light modulator, Pockels cells (Conoptics Inc.). All electrophysiological data were acquired by multiclump 700B amplifier (Axon Instruments), and signals were digitized at 10 kHz and low pass-filtered at 2 kHz.

A

		# of object measured in each condition			Tested dose (nM)		
		spine	dendrite	neuron	FRAX120	FRAX355	FRAX486
Prophylactic paradigm (Fig 4)	1st trial	240-573	18-27	6-8	125, 500, 2000	63, 250, 1000	125, 500, 2000
	2nd trial	265-835	12-27	5-14	125, 500, 2000	63, 250, 1000	125, 500, 2000
	3rd trial	126-432	9-24	5-8	2, 20, 125	2, 20, 63	2, 20, 125
Treatment paradigm (Fig 5)	1st trial	94-375	18-25	7-10	125, 500, 2000	63, 250, 1000	125, 500, 2000
	2nd trial	147-329	14-18	7-9	2, 20, 125	2, 20, 63	2, 20, 125

B Prophylactic paradigm

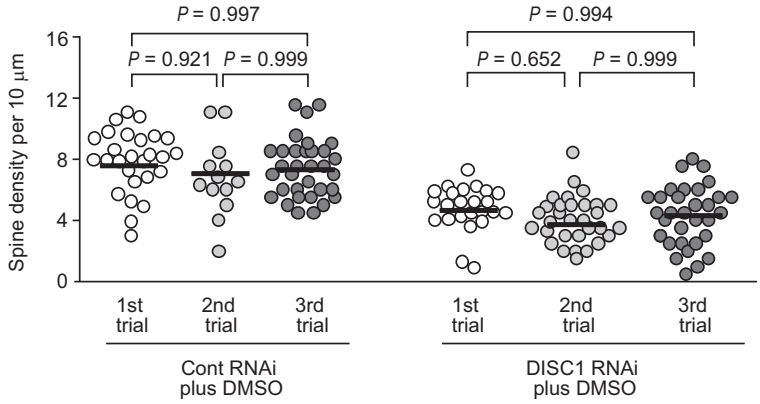

C Treatment paradigm

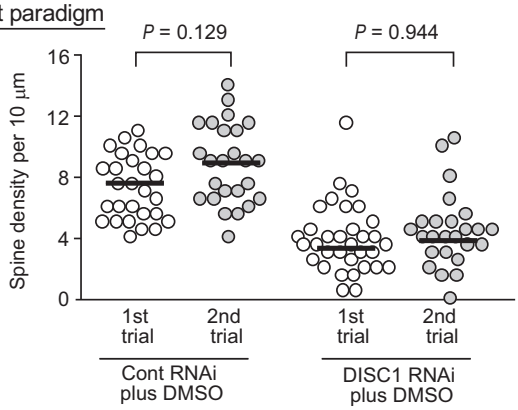

Fig. S1. Characteristics of experimental cohort used for each experiment. (*A*) Number of spines, dendrites, and neurons used for assays. The dose of p21-activated kinase (PAK) inhibitors (FRAX120, FRAX355, or FRAX486) assayed in each experiment is shown. (*B* and *C*) Scatter plots showing comparison of basal conditions among different cohorts. Spine densities of control RNAi plus DMSO indicate resilience of neurons, and those of Disrupted-in-Schizophrenia-1 (DISC1) RNAi plus DMSO indicate the knockdown efficiency of each experiment. The average and deviation of all three cohorts are quite comparable, which is supported by statistical analysis.

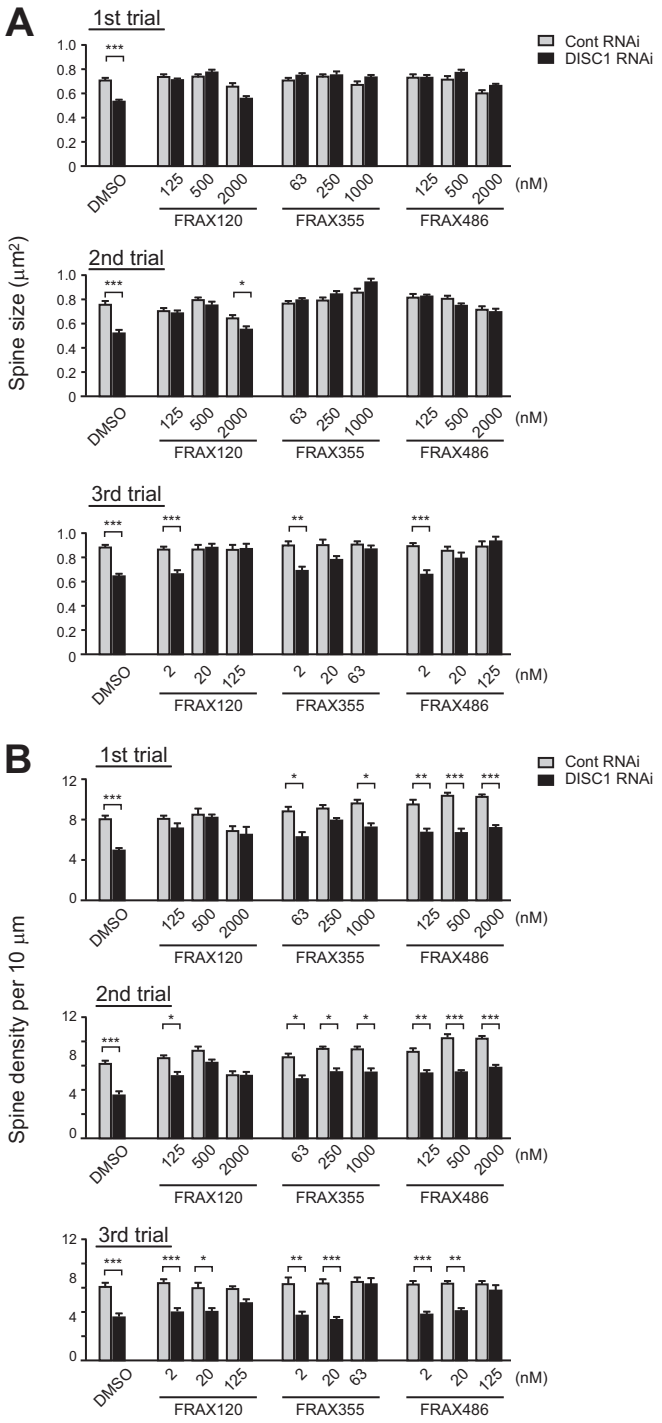

Fig. S2. Spine area size (*A*) and spine density (*B*) for each cohort of prophylactic paradigm. Identical doses of inhibitors were used for the first and second trials, demonstrating almost identical results. Efficacy of PAK inhibitors at the low dose range was assayed as the third trial. Combined data for all three cohorts data are shown in Fig. 3. $*P < 0.05$, $**P < 0.01$, and $***P < 0.001$.

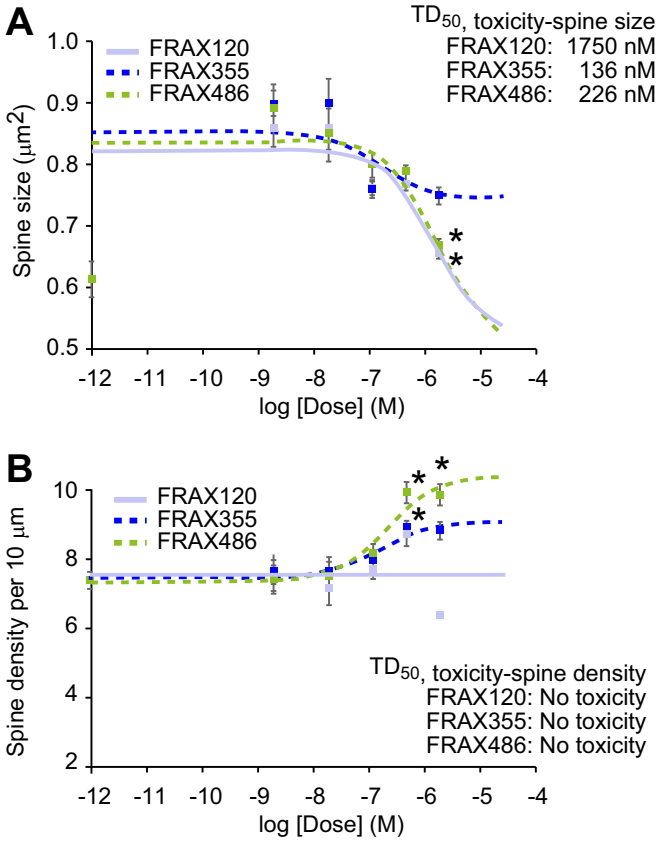

Fig. S3. Potential toxicity of PAK inhibitors on spine morphology under control conditions is shown (prophylactic paradigm). PAK inhibitors or vehicle were added at the time of transfection for control RNAi and incubated for 6 d before morphological analysis for the spine area size (*A*) and spine density (*B*). Asterisks indicate the significant difference between the spines with vehicle control and those with PAK inhibitors at each dose. Some adverse effects were observed only at doses more than a hundred times higher than the effective doses for synaptic protection against DISC1 RNAi (Fig. 3), suggesting that these PAK inhibitors had minimal effects on healthy spines. $*P < 0.05$. Dotted line indicates the average of the spine characteristics in neurons with control RNAi. Veh, only vehicle; TD_{50}, median toxic dose of 50%.

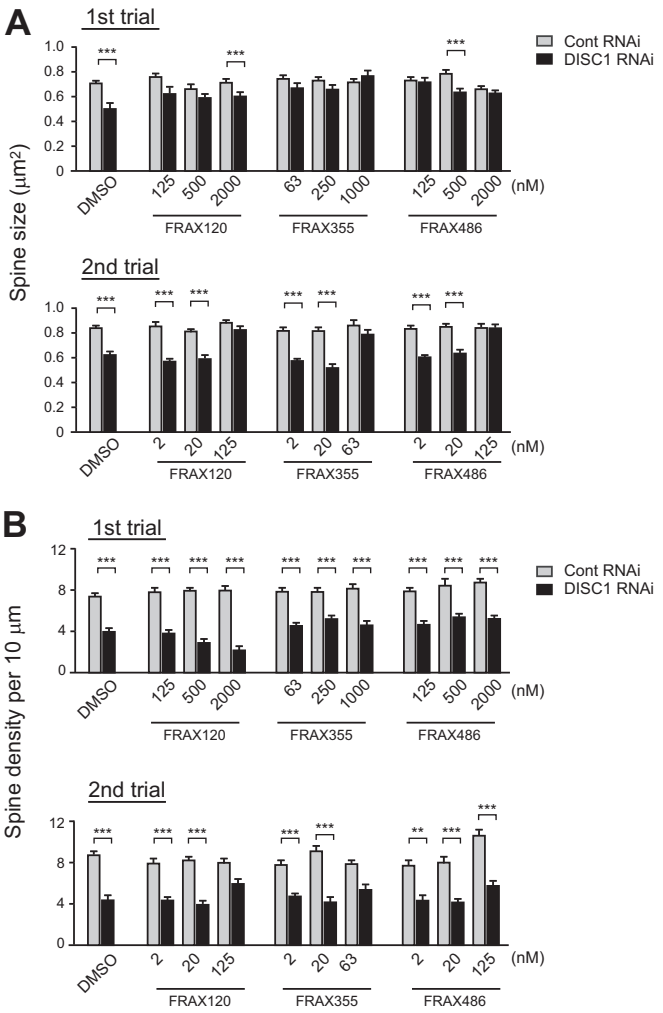

Fig. S4. Spine area size (*A*) and spine density (*B*) for each cohort of treatment paradigm. Efficacies of PAK inhibitors at the high dose range and low dose range were assayed as the first and the second trials, respectively. Combined data for these cohorts are shown in Fig. 4. ***$P < 0.001$.

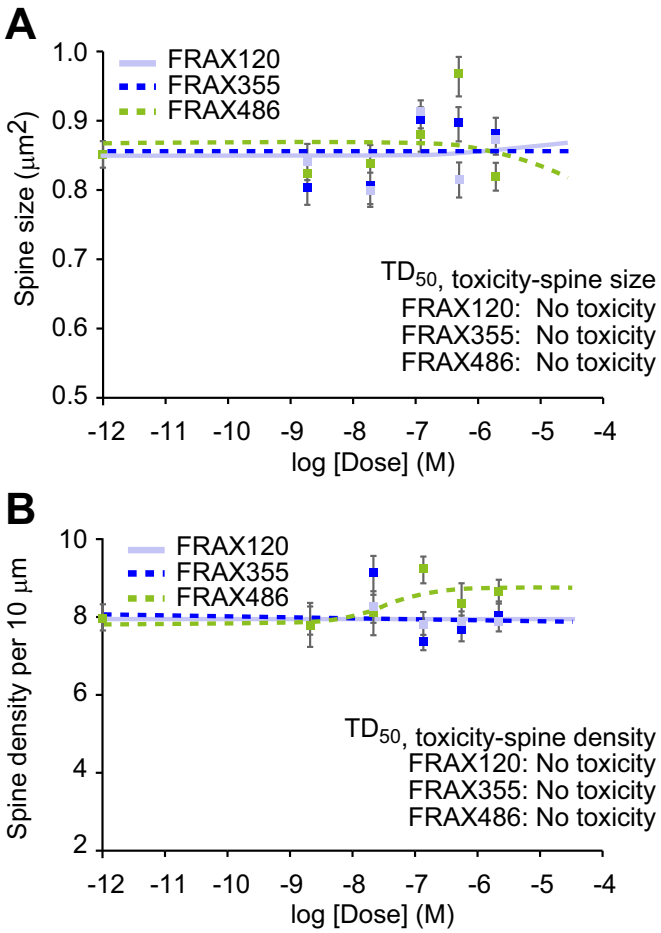

Fig. S5. Potential toxicity of PAK inhibitors on spine morphology in the control condition is shown (treatment paradigm). PAK inhibitors were added 5 d after the transfection of control RNAi, followed by 3 d incubation before morphological analysis for the spine area size (*A*) and spine density (*B*). Dotted line indicates the average of the spine characteristics in neurons with control RNAi. TD_{50}, median toxic dose of 50%.

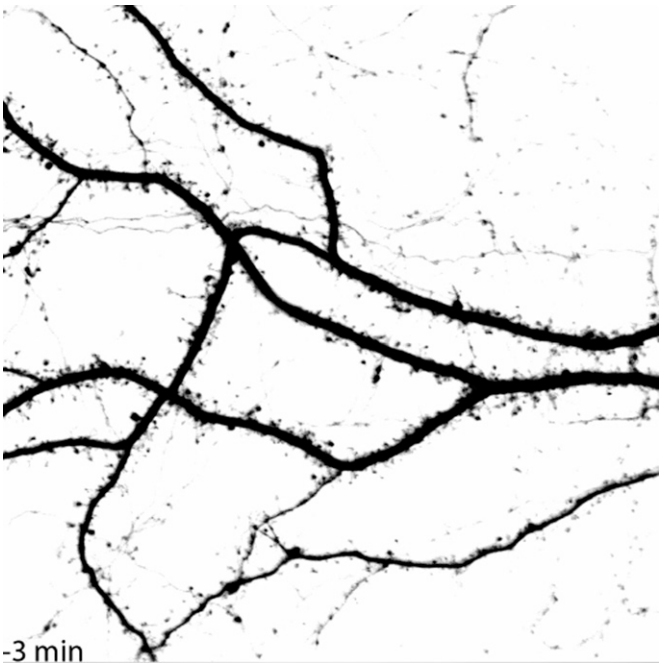

Movie S1. Primary cortical neuron culture pretreated with control shRNA was subjected to APV withdrawal treatment to induce the NMDA-R activation, and spine structural change was assessed by time lapse imaging. The majority of the spines were enlarged upon NMDA-R activation.

Movie S1

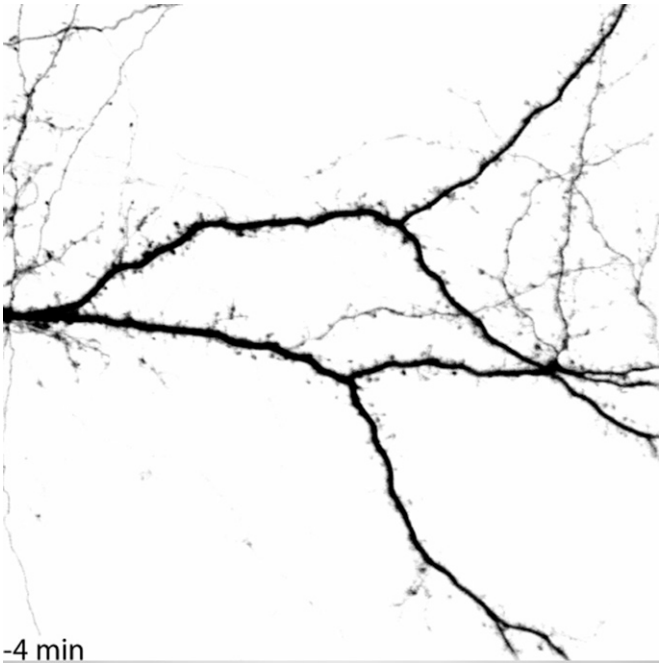

Movie S2. The spines in neurons pretreated with DISC1 shRNA displayed gradual shrinkage upon APV withdrawal treatment, which usually triggers the spine enlargement (Movie S1).

Movie S2